

Estimating the effects of increased urbanization on surface meteorology and ozone concentrations in the New York City metropolitan region

Kevin Civerolo^{a,*}, Christian Hogrefe^{a,b}, Barry Lynn^{c,d}, Joyce Rosenthal^e,
Jia-Yeong Ku^a, William Solecki^f, Jennifer Cox^f, Christopher Small^g,
Cynthia Rosenzweig^c, Richard Goldberg^c, Kim Knowlton^h, Patrick Kinney^h

^aNew York State Department of Environmental Conservation, Division of Air Resources, Albany, NY, USA

^bAtmospheric Sciences Research Center, Albany, NY, USA

^cNASA Goddard Institute for Space Studies, New York, NY, USA

^dCenter for Climate Systems Research, Earth Institute at Columbia University, New York, NY, USA

^eGraduate School of Architecture, Planning & Preservation, Columbia University, NY, USA

^fDepartment of Geography, Hunter College, New York, NY, USA

^gLamont-Doherty Earth Observatory of Columbia University, Palisades, NY, USA

^hMailman School of Public Health, Columbia University, New York, NY, USA

Received 26 January 2006; received in revised form 30 October 2006; accepted 31 October 2006

Abstract

Land use and pollutant emission changes can have significant impacts on air quality, regional climate, and human health. Here we describe a modeling study aimed at quantifying the potential effects of extensive changes in urban land cover in the New York City (NYC), USA metropolitan region on surface meteorology and ozone (O₃) concentrations. The SLEUTH land-use change model was used to extrapolate urban land cover over this region from “present-day” (ca. 1990) conditions to a future year (ca. 2050), and these projections were subsequently integrated into meteorological and air quality simulations. The development of the future-year land-use scenario followed the narrative of the “A2” scenario described by the Intergovernmental Panel on Climate Change (IPCC), but was restricted to the greater NYC area. The modeling system consists of the Penn State/NCAR MM5 mesoscale meteorological model; the Sparse Matrix Operator Kernel Emissions processing system; and the US EPA Community Multiscale Air Quality model, and simulations were performed for two 18-day episodes, one near-past and one future. Our results suggest that extensive urban growth in the NYC metropolitan area has the potential to increase afternoon near-surface temperatures by more than 0.6 °C and planetary boundary layer (PBL) heights by more than 150 m, as well as decrease water vapor mixing ratio by more than 0.6 g kg⁻¹, across the NYC metropolitan area, with the areal extent of all of these changes generally coinciding with the area of increased urbanization. On the other hand, the impacts of these land use changes on ozone concentrations are more complex. Simulation results indicate that future changes in urbanization, with emissions held constant, may lead to increases in episode-average O₃ levels by about 1–5 ppb, and episode-maximum 8 h O₃ levels by more than 6 ppb across much of the NYC area. However, spatial patterns of ozone changes are heterogeneous and also indicate the presence of areas with decreasing ozone concentrations. When anthropogenic emissions were increased to be consistent with the

*Corresponding author. Tel.: +1 518 402 8383; fax: +1 518 402 9035.

E-mail address: kxcivero@gw.dec.state.ny.us (K. Civerolo).

extensive urbanization in the greater NYC area, the O₃ levels increased in outer counties of the metropolitan region but decreased in others, including coastal Connecticut and the Long Island Sound area.

© 2006 Elsevier Ltd. All rights reserved.

Keywords: Models-3/CMAQ; MM5; Air pollution meteorology; O₃; Land use change

1. Introduction

The greater New York City (NYC), USA metropolitan region covers parts of the states of New York, New Jersey, and Connecticut and currently has a population exceeding 21 million. Ongoing urbanization in this area puts a significant strain on natural resources and impacts air pollution levels and regional climate. As more land in this region is expected to be converted from natural and vegetated land cover to human-dominated uses over the coming decades, it is of interest to predict the concomitant effects on public health and welfare. To assess such impacts under different scenarios of future conditions, it is necessary to integrate a diverse set of modeling tools across a range of spatial and temporal scales, from the global scale (general circulation models (GCM)) to the regional scale (mesoscale meteorology and air quality models) to local and urban scales (high resolution meteorology, air quality, and health impacts models). A goal of the New York Climate & Health Project (NYCHP; Kinney et al., 2006) was to develop and apply such a modeling framework across the New York City region.

There have been several studies of the NYC region that have described some of these model linkages. Lynn et al. (2004, 2006) described the integration of a global climate model with that of regional meteorology that serves as a foundation for this and related studies. Hogrefe et al. (2004a) examined the effects of changes in global and regional climate and emissions on air quality over the eastern United States, comparing simulated O₃ concentrations from five summers of the 2050s with those of the 1990s. Hogrefe et al. (2004a) found that intercontinental transport of O₃ and precursors, increasing regional emissions of O₃ precursors, and CO₂-induced changes to meteorological variables such as temperature, boundary layer heights, and synoptic flow patterns all have the potential to affect future attainment of ambient air quality standards. Using the climate and air quality results from that study, Knowlton et al. (2004) estimated the potential changes in summertime O₃-related

mortality across the metropolitan area over the same time period. The increase in regionally aggregated mortality due to climate change alone was found to be similar to that of coupled climate change and increases in O₃ precursors, and possible increases in regional precursor emissions were found to cause higher increases in mortality rates in the outlying suburban counties.

In those four studies, the regional meteorology and air quality simulations were generated at 36 km grid resolution, land use was held constant in all simulations, and mortality rates were projected to the county level. Here, we describe an approach to incorporate detailed (~70 m) land cover information into high-resolution (4 km) meteorological and photochemical model simulations around NYC. We then utilize this approach to assess the relative roles of future increased urban land cover and associated changes in emissions on surface level meteorological fields and O₃ concentrations. Additionally, we discuss these land-use-induced changes in surface-level meteorology and ozone in the context of possible changes caused by changing emissions.

2. Modeling system

2.1. Urban land cover modeling

Solecki and Oliveri (2004) described the development of two sets of detailed land cover information for the greater NYC metropolitan area, namely “current” conditions and estimated land cover by the middle of the 21st century. First, the authors established the current (ca. 1990) distribution of wetlands, water, barren, forest, agriculture, rangeland, and urban land cover across the greater NYC metropolitan area at 70 m resolution (for a map of this region, please see <http://www.geography.hunter.cuny.edu/luca/Home/Overview.html>).

To generate the ca. 2050 land cover database, the slope, land-use, exclusion, urban extent, transportation, hillshade (SLEUTH) model (Clarke et al., 1997) was used to estimate the potential impacts of urban growth over the next five decades (Solecki

and Oliveri, 2004). SLEUTH makes projections of land cover change based upon growth-inducing variables that include slope, land cover/use, exclusion zones (i.e. parks and conservation areas), and proximity to transportation infrastructure; growth parameters based on recent patterns of urbanization; and additional growth rules. SLEUTH has been used to describe urban growth in the San Francisco Bay region (e.g. Clarke et al., 1997) and to assess the effects of increased urban development in the Baltimore, Maryland/Washington, DC region on the Chesapeake Bay watershed (e.g. Claggett et al., 2004). Before performing the future year simulation, SLEUTH was calibrated to “current” conditions using growth patterns from the USGS Urban Dynamics Research Program (please see <http://landcover.usgs.gov/LCI/urban/intro.php>) for the greater NYC region from 1960 to 1990, including urban/non-urban designations in 1960, 1970, 1980, and 1990, and land cover (urban, agricultural, forest, grassland, wetland, water, and barren land) in 1975 and 1992.

The SLEUTH model consists of two sub-models, the urban growth model (UGM) and the land cover deltatron model (LCDM). The UGM estimates the probability that a given non-urban grid cell will be converted to urban in the future, while the LCDM specifies which type of non-urban land type can be converted to urban. Solecki and Oliveri (2004) used the UGM and LCDM to generate future land cover in the greater NYC region for the year 2050 consistent with the narrative of the Intergovernmental Panel on Climate Change (IPCC) special report on emissions scenarios (SRES) “A2” emissions scenario (please see <http://www.ipcc.ch/pub/sres-e.pdf>). The A2 scenario predicts large increases in greenhouse gas emissions, relatively weak environmental concerns, and large population growth away from existing urban centers, i.e. new urban growth will tend to occur in areas previously considered open space. This is only one of several IPCC climate change and emissions scenarios, albeit a fairly pessimistic one, that we chose as a worst-case scenario of urban sprawl and increased anthropogenic emissions (including an IPCC-estimated CO₂ emissions increase of ~50%). It is important to reiterate that for the current study, SLEUTH predictions of future-year land use were only available for the greater NYC area, not for the entire modeling domain as described in Sections 2.2–2.4. Clearly, it would be desirable to generate future-year land use information for larger geo-

graphic areas, but this was beyond the scope of our study.

The urban land for this future year scenario was further subdivided into three separate categories, namely high density, medium density, and low density urban. This classification scheme was developed from the 1990s land use categories and remotely-sensed vegetative fraction (VF) from Landsat imagery for the greater NYC region plus most of New Jersey and Connecticut (Pozzi and Small, 2005). Specifically, high density urban was defined as having $VF < 22\%$; medium density urban, $22\% < VF < 51\%$; and low density urban, $VF > 51\%$. All future urban growth predicted by SLEUTH for the greater NYC metropolitan area was assumed to be low density urban, i.e. suburban, residential, or employment-based development away from the core urban center. Grid cells within the greater NYC metropolitan area that were classified as urban in both the 1990s and 2050s simulations were assigned the appropriate urban category derived from the 1990s classification. Fig. 1a shows the three urban land use categories simulated by SLEUTH for the 2050s. Section 2.2 contains additional details on how this high-resolution future year land cover was subsequently incorporated into the meteorological model.

2.2. Meteorological modeling and episode selection

The non-hydrostatic fifth-generation mesoscale model (MM5) version 3.5 (Dudhia, 1993; Grell et al., 1994) was the regional-scale meteorological model. The MM5 was developed by the Pennsylvania State University and National Center for Atmospheric Research and simulates three-dimensional wind components, temperature, mixing ratios for water vapor, and cloud water/ice and rain/snow. Thirty-five vertical layers were used, with finer grid resolution in the lower troposphere to allow the model to simulate boundary-layer processes more realistically. The $4^\circ \times 5^\circ$ NASA Goddard Institute for Space Studies Global Circulation Model (GISS-GCM; Russell et al., 1995) provided initial conditions and lateral and surface boundary fields for MM5. Hogrefe et al. (2004a, b) and Lynn et al. (2004, 2006) performed the coupled GISS-GCM/MM5 simulations for five summers during the 1990s (1993–1997) and 2050s (2053–2057) at horizontal grid resolutions of 108 and 36 km. The MM5 simulations from the 2050s are forced by climate change as predicted by the GISS-CGM and A2

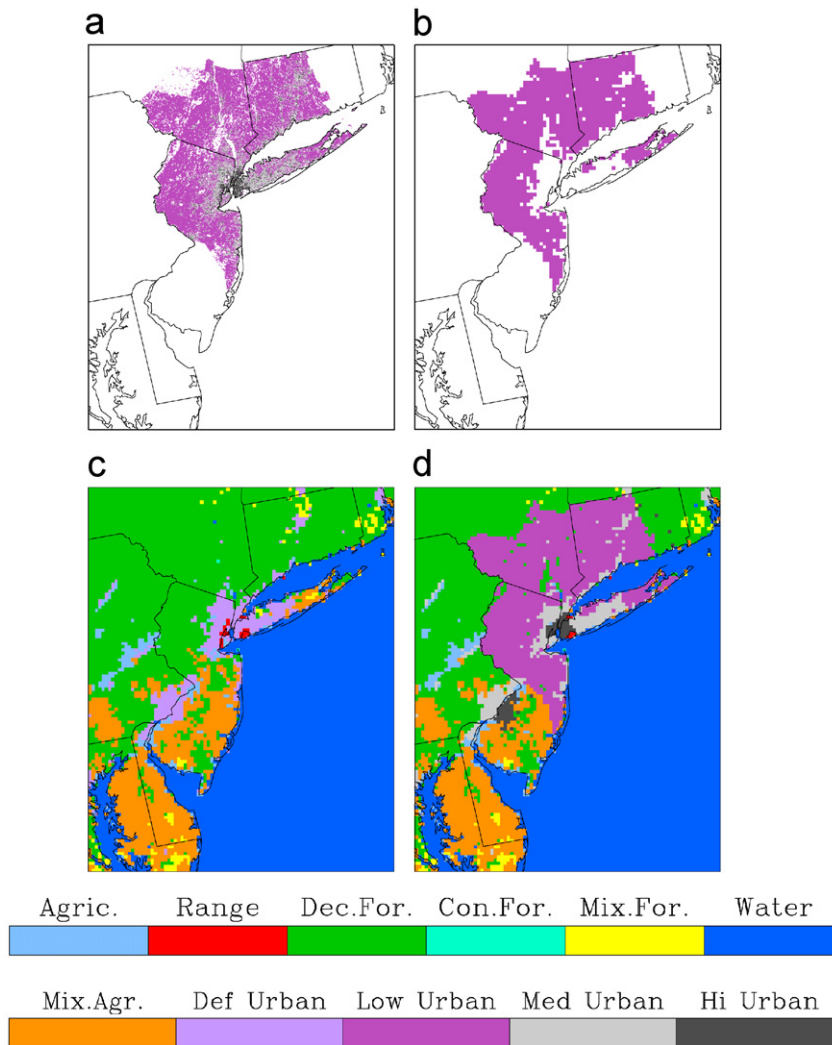


Fig. 1. (a) The three urban land use categories—low density (purple), medium density (light gray)—simulated by SLEUTH for the 2050s. (b) The 4 km MM5 grid cells converted from non-urban in the 1990s to low density urban in the 2050s by SLEUTH (c) The default 4 km MM5 land use in the 1990s (d) The 4 km MM5 land use in the 2050s.

scenario discussed in Section 2.1; for example, surface temperatures from the five-summer 36 km MM5 simulations were on average $\sim 2^\circ\text{C}$ warmer in the 2050s than 1990s (Hogrefe et al., 2004a; Lynn et al., 2006).

For this study, MM5 simulations at a horizontal resolution of 4 km were generated in a two-step approach. First, the 108 km MM5 fields (Lynn et al., 2004) were used to initialize and provide lateral boundary conditions for the 36 and 12 km two-way interactive nested domains. Six-hourly GISS-GCM temperature, wind, pressure, and moisture fields were interpolated to the lateral boundaries of the 108 km MM5, and a five-point linear time

interpolation was used to make the lateral boundary data synchronous with the MM5 time steps, following Davies and Turner (1977). Each simulation was run from May 1 to September 30. Starting the model in May allows the atmospheric component of the mesoscale model ample time to “spin-up” before the start of the analysis on June 1 in each summer. One month of spin-up was used to establish an equilibrium between the lateral and surface boundary conditions and MM5-simulated fields, especially an equilibrium between rainfall and soil moisture. In contrast, the soil temperature and moisture distribution from the GISS-GCM acts like a time-varying bottom boundary condition during the development

of summertime meteorology (Dirmeyer, 2003). The concentration of CO₂ used in the MM5 was modified in the 2050s run to be consistent with the GISS-GCM, since atmospheric CO₂ levels affect the radiation calculations; this modification was not made in the 1990s run which reflects current CO₂ levels.

To obtain the high-resolution meteorology for this study, the 4 km simulation (see Fig. 1 for approximate domain extent) was generated using the output from the 12 km grid as initial and boundary conditions. Note that the SLEUTH domain covers only the greater NYC metropolitan area, whereas the meteorological and photochemical modeling domain extends from the mid-Atlantic seaboard to southern New England. Two 18 day periods were chosen during the summers of 1993 (July 5–22) and 2056 (June 17–July 4), since these periods experienced episodes of extremely high surface temperatures and O₃ levels across the metropolitan region in the 36 km model simulations. Specifically, both the episode average and episode maximum ranked at the 98th percentile of 18 day average and daily maximum temperature and daily maximum hourly O₃ from the two five-summer 36 km simulations mentioned above. After these periods were chosen and the 4 km simulations performed, analysis was conducted to confirm that only minor differences existed in the spatially-averaged temperatures between the 36 and 4 km simulations across the area of overlap. In other words, the higher grid resolution did not introduce any systematic warming or cooling effect, i.e. these two episodes still represent extremely warm conditions at the higher grid resolution. It should be noted, however, that the 2056 episode is not necessarily representative of the “same” period in 1993.

The land surface model used in the MM5 simulations was that of Chen and Dudhia

(2001a, b). The default land cover for the MM5 domain is based upon the 25-category USGS thematic vegetation/land use data. In this study the default land cover database was used for the current land use simulations, as it best reflects current conditions consistent with the MM5 parameterizations across the model domain, while the input land use was modified based on the SLEUTH results for the future land use simulations. For this purpose, we assigned each 70 m SLEUTH “pixel” to the appropriate 4 km MM5 grid cell, and then determined the dominant SLEUTH category in each 4 km grid cell for the 1993 and 2056 episodes. If the dominant category was one of the three urban designations described in Section 2.1, we replaced the default MM5 land cover from the current land use simulations with that computed from the SLEUTH results; otherwise, we retained the default MM5 land use. Table 1 lists the physical parameters used to characterize the three new urban categories, and land cover types that do not appear in this model domain in the landuse look-up table (LANDUSE.TBL) were modified to allow for these new urban types. Note that albedo and roughness length are also set in the subroutine that defines the vegetation parameters for a given vegetation type (prmvveg_usgs.F) in the land surface model; this routine was modified to be consistent with the values defined in LANDUSE.TBL. These urban land use types are assumed to be a mixture of grass, deciduous tree, and impervious surface, and the values in Table 1 represent weighted averages of these parameters for these three categories based on assumed fractional coverage (Luley and Bond, 2002), namely: high density, 34% grass/14% tree/53% impervious; medium density, 16% grass/25% tree/59% impervious; and low density, 35% grass/33% tree/32% impervious. Note that the new medium density urban category is identical to the default urban category in MM5. These fractional

Table 1
Surface parameter values for the landuse look-up table in MM5 for the three urban categories

Urban type	Shortwave albedo (%)	Moisture availability (%)	Longwave emissivity (%)	Surface roughness (cm)	Thermal inertia (cal cm ⁻² K ⁻¹ s ^{-1/2})	Surface heat capacity (J m ⁻³ s ⁻¹)
High	17	10	88	100	0.03	18.7 × 10 ⁵
Medium	18	10	88	50	0.03	18.9 × 10 ⁵
Low	18	15	90	30	0.03	20.6 × 10 ⁵

These parameter values represent weighted averages based on the differing amounts of grass, deciduous tree, and impervious surface percent cover from Luley and Bond (2002).

coverages were also used in the land surface model; surface resistances for grass, deciduous trees, and impervious surfaces were computed separately and then weighted according to these percentages for the three urban land types.

For all urban grids beyond the SLEUTH domain (i.e. outside of the greater NYC region), the parameter values corresponding to the medium density category were used in the future land use simulations. All non-urban grid cells (water, deciduous or coniferous forest, agriculture, etc.) within the MM5 domain retained the default MM5 land use. Fig. 1b shows only those low density urban grid cells converted from non-urban to urban between the 1990s and 2050s, while Figs. 1c and d display all land use categories used in the current and future land use simulations, respectively.

The SLEUTH domain is considerably smaller than the MM5 domain, and, as stated in Section 2.1, this study does not address urban growth outside of the NYC metropolitan area. In other words, we focus on urbanization in the immediate NYC region only, and have not assessed the effects of potential urban growth in upwind areas that could also have an impact on the NYC area. Note, too, that the introduction of three urban land use types in the future year simulations, compared to one in the current year simulations does introduce a slight inconsistency between the simulations. For example, in the Philadelphia metropolitan area, the New Jersey portion (which is within the SLEUTH domain) is classified as high density urban in the future year, while the Pennsylvania side is not, since it falls outside of the SLEUTH domain (see Fig. 1d).

2.3. Emissions processing

The anthropogenic emission inventory utilized for this study was the county-level United States Environmental Protection Agency (US EPA 1996 National Emissions Trends, NET96) inventory. This emission inventory was processed by the Sparse Matrix Operator Kernel Emissions Modeling System (SMOKE) Version 2.1 (Houyoux et al., 2000; Carolina Environmental Programs, 2003) to obtain gridded, hourly speciated emission inputs for the air quality model. Mobile source emissions were estimated by the Mobile5b model (United States Environmental Protection Agency (US EPA), 1994) integrated into SMOKE. Biogenic emissions were estimated with the Biogenic Emissions Inventory

System—Version 2 (BEIS2) model that takes into account the effects of temperature and solar radiation on the rates of these emissions (Geron et al., 1994; Williams et al., 1992).

For some of the sensitivity simulations described below, an attempt was made to modify anthropogenic and biogenic emissions to be consistent with the future year land use pattern simulated by SLEUTH and utilized for some of the MM5 simulations. For the biogenic emissions, the land use database utilized by BEIS2 was modified to be consistent with the projected changes in future urban land use. For those 4 km grid cells in which SLEUTH predicted an increase in urban land use from the base case, the agricultural and forest fractions in the biogenic emission land use database were reduced by a corresponding amount.

Estimates of future anthropogenic emissions, such as those projected by the IPCC, are useful on a countrywide or continental basis, but they do not provide detailed future year emissions specific to the greater NYC metropolitan area. To estimate future anthropogenic emissions consistent with the 2050 A2 land use predictions, we relied on the current gridded anthropogenic emissions and SLEUTH database to determine urban land use fraction in each model grid cell. In the current SLEUTH database, each grid cell consists of different amounts of tree, grass, and impervious surfaces. Knowing the impervious cover fraction in each grid cell, we were able to derive an empirical relationship between urban land use fraction and anthropogenic emissions:

- For the current land use scenario, the ratio of SMOKE-processed gridded anthropogenic emissions between any pair of non-water grid cells is correlated with the ratio of urban land use percentages between the same two grid cells. To demonstrate that this assumption is valid at least to first order, Fig. 2a and b show box plots and a best fit through the medians for the ratio of anthropogenic NO_x emissions vs. the ratio of urban fractions for all pairs of grid cells in the modeling domain.
- Determining the functional form of the best-fit line of the medians and performing this analysis for volatile organic compounds (VOC), NO_x , and CO from the base case scenario, one can then utilize this relationship to determine the future year scaling ratio for each grid cell based on the SLEUTH-predicted change in urban land use

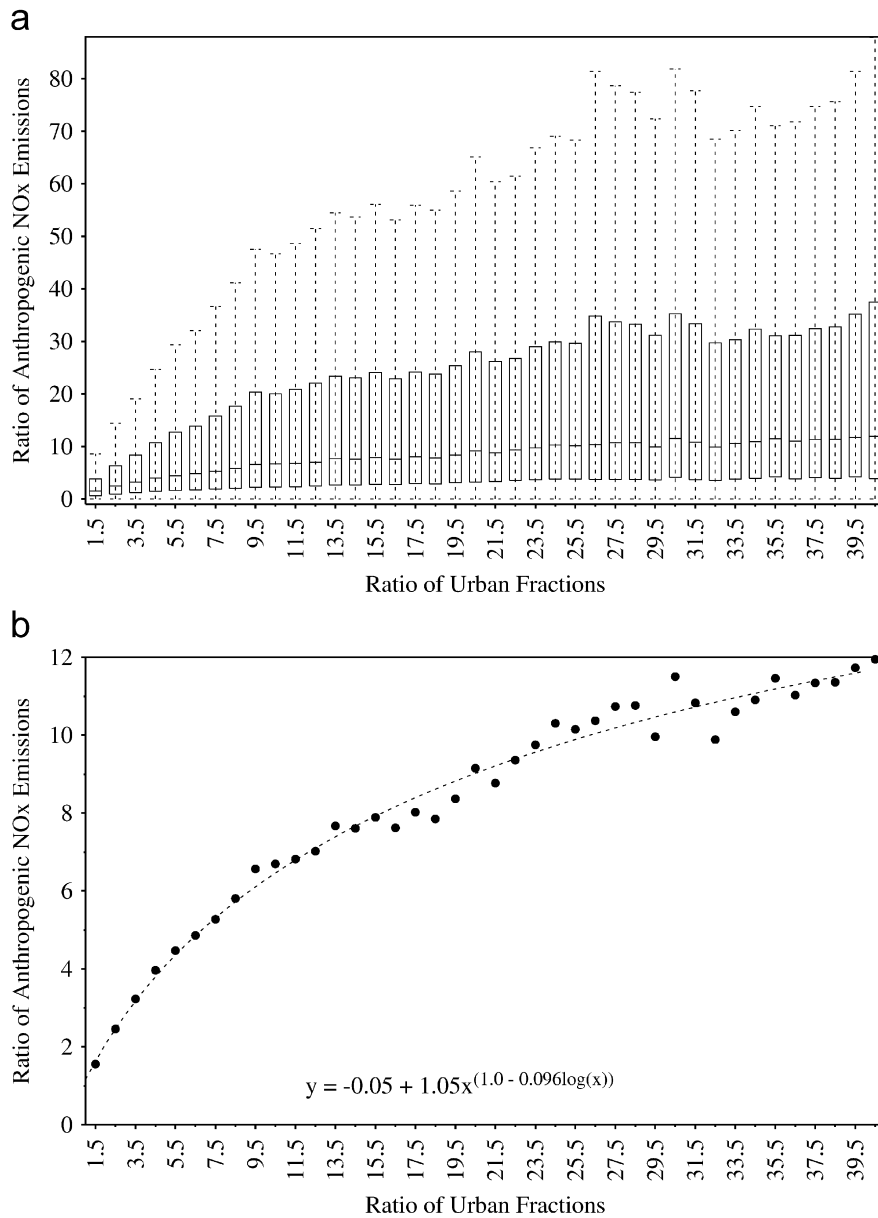


Fig. 2. Ratio of anthropogenic NO_x emissions vs. the ratio of urban fractions for all pairs of grid cells in the modeling domain: (a) box and whisker plot displaying the median, inter-quartile range (IQR), and $\pm 1.5 \times \text{IQR}$ bounds; and (b) median values with a best fit curve.

percentage (i.e. the ratio of future urban area over current urban area for each grid cell).

- Lastly, anthropogenic emissions consistent with future land use can be estimated by multiplying the gridded base case emissions with these gridded scaling ratios.

By applying this methodology, we estimated anthropogenic emissions consistent with the future

year land use patterns. Table 2 shows a summary of anthropogenic and biogenic emissions for the current and future land use scenarios for a typical weekday, over the greater NYC region. Not surprisingly, it can be seen that increased urbanization results in a decrease of biogenic emissions and an increase of anthropogenic emissions. It should be noted that the estimates of future emissions do not take into account possible changes in emission

factors, transportation patterns, or technology, as none of this information was available for this study. However, these estimates do provide a rough sensitivity of the emission totals and spatial distributions consistent with increased urbanization given today's technology and transportation and travel behavior.

2.4. Air quality modeling

Using the SMOKE-processed emissions and the 4 km MM5 regional climate simulations for the two 18 day episodes in the model years 1993 and 2056 described above, air quality simulations were performed using the Models-3/community multi-scale air quality (CMAQ) model Version 4.2 (Byun and Schere, 2006). Initial and boundary conditions for these simulations were derived from the 12 km CMAQ simulations nested within the 36 km MM5/CMAQ simulations for the same time period described in Hogrefe et al. (2004a). The 4 km CMAQ modeling domain used in this study is depicted in Fig. 1 and is identical to the MM5 modeling domain, except for the removal of MM5 boundary cells. Sixteen vertical layers were utilized in CMAQ, with all layers below 3 km being identical to the MM5 vertical structure, while mass-averaging was used to perform layer-collapsing for layers

above 3 km. The carbon bond IV mechanism (CB-IV; Gery et al., 1989) was used to simulate gas-phase chemistry. The CMAQ model has undergone extensive community development and peer review and has been used successfully for a number of regional air quality studies (e.g. Bell and Ellis, 2003, 2004; Binkowski and Roselle, 2003; Hogrefe et al., 2004a, b; Ku et al., 2001; Mebust et al., 2003; Tong and Mauzerall, 2006). In this study, we performed the six CMAQ simulations listed in Table 3 to study the effects of: current (ca. 1990s) emissions and land cover with two different meteorological episodes (simulations 1 and 4) to provide a sense of natural variability and/or a changing climate; increasing urban land cover in the NYC region consistent with the A2 scenario without changing emissions (simulations 2 and 5); and the combined effects of increased urban land cover and emissions (simulations 3 and 6).

3. Results

3.1. Impact of increased urbanization on surface meteorology

To investigate the impact of changed land use on surface meteorology, here we focus primarily on three parameters: air temperature, PBL heights, and water vapor mixing ratios because these variables have a significant impact on surface O₃ concentrations (Aw and Kleeman, 2003; Gaza, 1998; National Research Council, 1991; Rao et al., 2003). The largest changes (defined as “future-base”) in surface meteorology tended to occur over the extended metropolitan area away from the core urban areas, corresponding to regions with the largest urban growth potential (see Figs. 3a–f) for the 1993 and 2056 episodes. Figs. 3a, c and e reflect the differences between simulations 1 and 2, while Figs. 3b, d, and f reflect the differences between

Table 2

Domain-wide anthropogenic (carbon monoxide (CO), nitrogen oxides (NO_x), and volatile organic compounds (VOC)) and biogenic (isoprene) emissions in tons day⁻¹ for the base and future land use scenarios for a typical weekday, summed over the 31-county New York City CMSA

	1990 Base land use	2050 A2 land use
CO (anthropogenic)	10,920	17,024
NO _x (anthropogenic)	2133	3446
VOC (anthropogenic)	2490	3749
Isoprene (biogenic)	734	251

Table 3

The six MM5/CMAQ simulations

Simulation number	Simulation description	Meteorology	Emissions	Land use
1	1993 “Base” episode	July 5–22, 1993	1996 Base	1990 Base
2	1993 Episode, A2 land cover	July 5–22, 1993	1996 Base	2050 A2
3	1993 Episode, A2 land cover and emissions	July 5–22, 1993	Consistent with 2050 A2	2050 A2
4	2056 “Base” episode	June 17–July 4, 2056	1996 Base	1990 Base
5	2056 Episode, A2 land cover	June 17–July 4, 2056	1996 Base	2050 A2
6	2056 Episode, A2 land cover and emissions	June 17–July 4, 2056	Consistent with 2050 A2	2050 A2

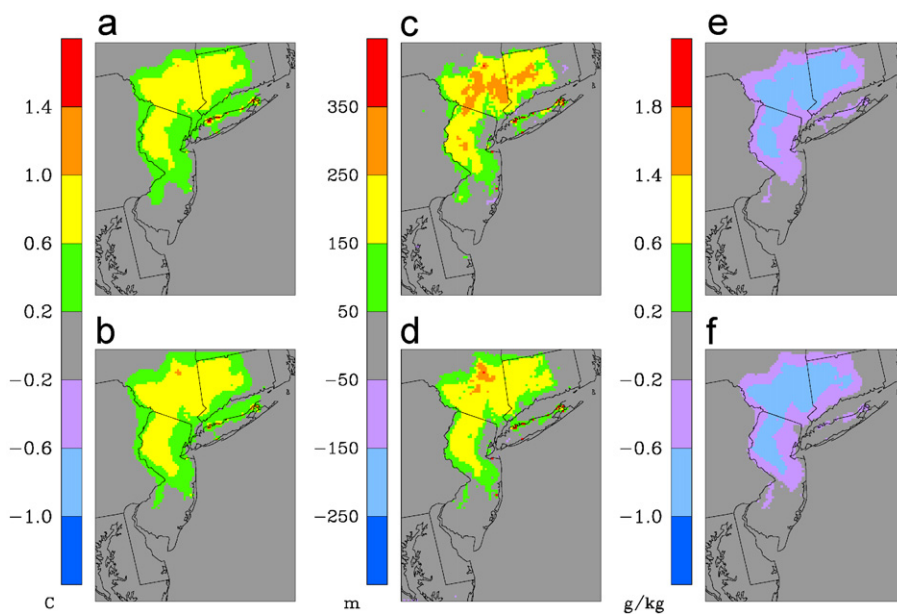


Fig. 3. Differences in afternoon (12–18 EST) average surface meteorological fields for the 1993 and 2056 episodes, defined as “future-base” urban land cover: (a) temperature, 1993 episode; (b) temperature, 2056 episode; (c) PBL height, 1993 episode; (d) PBL height, 2056 episode; (e) water vapor mixing ratio, 1993 episode; and (f) water vapor mixing ratio, 2056 episode. Figs. 3a, c, and e reflect the differences between simulations 1 and 2, while Figs. 3b, d, and f reflect the differences between simulations 4 and 5.

simulations 4 and 5. Figs. 3a–f suggest that as a result of increased urban growth consistent with the A2 scenario, the daytime (12–18 EST) episode-average surface temperatures across the metropolitan area increased by more than 0.6°C ; PBL heights increased by more than 150 m; and surface water vapor mixing ratios decreased by more than 0.6 g kg^{-1} . The changes in surface meteorology are spatially very similar for the two meteorological episodes.

Although these two episodes are only 18 days long and, therefore, not sufficiently long to attribute differences between the episodes to climate change, such differences can provide a measure of meteorological variability and context for the observed changes resulting from increased urban land cover. In these simulations, the domain-wide daytime episode average surface temperatures over non-water grid cells were nearly identical for the two base episodes (25.93°C for simulation 1, 1993; 25.89°C for simulation 4, 2056). Although the overall average surface temperatures were nearly identical for the two episodes, there were differences in the spatial patterns (not shown here). For example, the 2053 (simulation 4) episode predicted temperatures $\sim 1^{\circ}\text{C}$ higher over Delmarva, and $\sim 1^{\circ}\text{C}$ cooler over southeastern Pennsylvania. The

1993 episode was substantially drier (9.26 g kg^{-1} vs. 11.79 g kg^{-1}), and average PBL heights were higher as well (1663 m vs. 1352 m). In terms of the domain-wide episode maximum values over non-water grid cells, the 1993 episode (simulation 1) was slightly cooler (30.41°C vs. 30.76°C), had slightly lower PBL heights (2071 m vs. 2125 m), and was substantially drier (15.04 g kg^{-1} vs. 16.79 g kg^{-1}). While the two episodes are similar in that they both experienced extreme surface temperatures, they do cover two different points in time separated by more than 60 years, and they are driven by two distinct GCM climate scenarios. Hence, they are not necessarily representative of the “same” period in time, and it is not unexpected that differences between simulations 1 and 4 exist in the absence of land use change.

These temperature changes are comparable to an earlier modeling study by Civerolo et al. (2000), in which $\sim 40\%$ of the area in the NYC metropolitan area originally classified as urban was re-classified as deciduous forest; away from the core downtown area, primarily in Long Island and along the Connecticut coast, the additional forest cover reduced near-surface temperatures by 1°C or more. The changes observed in this study are directionally consistent with the substantial increases in urban surfaces across large parts of the model domain, and the spatial pattern of

the meteorological changes generally matches the area of increased urbanization.

The future increased urban land cover also had a noticeable effect on surface layer winds across the metropolitan region, generally leading to an increased sea breeze along coastal Connecticut and Long Island, and increasing convergence over southeastern New York and central Connecticut. We did not examine winds in detail in this study, however, although transport certainly plays an important role on O_3 concentrations in this region.

3.2. Impact of increased urbanization and emissions changes on surface O_3

The previous national ambient air quality standard (NAAQS) for daily maximum O_3 in the US is 0.12 ppm (1 h average), whereas the current NAAQS is 0.08 ppm and is based on an 8 h average (please see <http://www.epa.gov/air/criteria.html>). Hence, we focused the subsequent 1 h analysis on those grid cells with daily maximum 1 h O_3 concentrations exceeding 124 ppb and daily maximum 8 h concentrations exceeding 84 ppb. Figs. 4a and b display the percentage of the non-water grid cells across the model domain in which the 1 h daily maximum O_3 concentration exceeded 124 ppb, and the 8 h daily maximum O_3 concentration exceeded 84 ppb, respectively. The percentage was calculated by dividing the total number of all exceedances of these thresholds at all grid cells over each of the two episodes by the product of all 18 episode days and all 5822 non-water grid cells (out of a possible 10,881). The numbers in the bar charts denote the six model simulations. For the 1993 episode, extensive urbanization across the NYC region led to a slight increase in the occurrence of high daily maximum 1 h O_3 concentrations (compare simulations 2 and 1, Fig. 4a). However, the additional increase in anthropogenic emissions consistent with the A2 scenario did not have an appreciable effect on the number of occurrences of high 1 h daily maximum values over land areas (compare simulations 3 and 2, Fig. 4a). In terms of 8 h daily maxima, the combined effects of future urban growth and increased anthropogenic emissions did lead to higher 8 h concentrations compared with just land use changes alone for the 1993 episode (Fig. 4b).

Fig. 4a also shows that there were roughly 2–3 times as many occurrences of high 1 h O_3 values for the 2056 episode over non-water grid cells than for the 1993 episode, regardless of emissions and urban

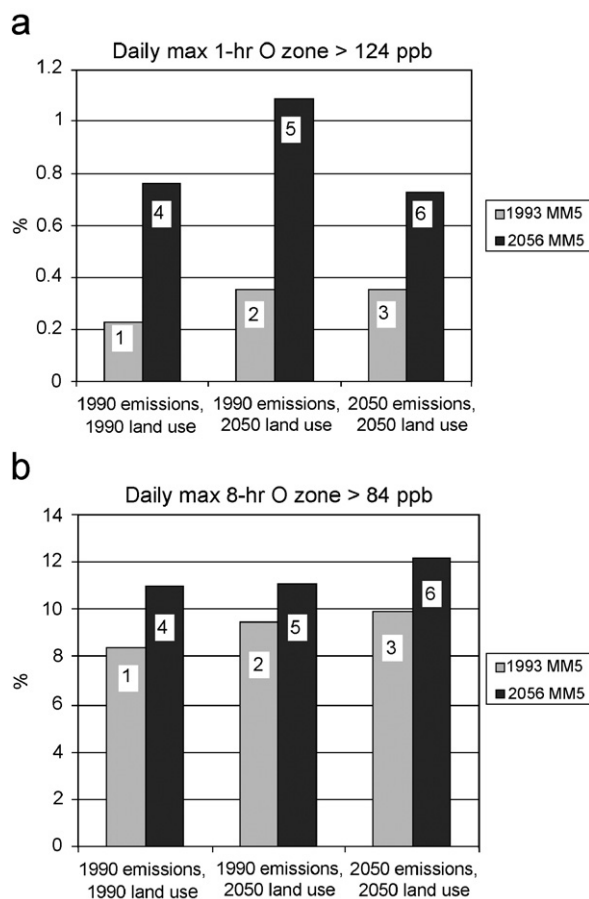


Fig. 4. (a) Histogram of daily maximum 1 h surface O_3 concentrations over non-water grid cells for the 1993 and 2056 episodes for the different CMAQ simulations. (b) Same as (a), except for daily maximum 8 h O_3 . The numbers in the bar charts refer to the different simulations.

land cover scenario. Unlike the 1993 episode, the combined effects of increased urbanization and increased emissions actually led to fewer occurrences of high 1 h O_3 concentrations than in the base 2056 episode (compare simulations 6 and 4, Fig. 4a), likely due to increased O_3 removal by titration caused by higher anthropogenic emissions in an already emissions-dense region. In terms of occurrences of high 8 h concentrations over land, the effects of urbanization alone were negligible domain-wide (compare simulations 5 and 4, Fig. 4b).

Table 4 lists the episode-average, standard deviation, and episode-maximum hourly O_3 concentrations from each of the six simulations, over non-water grid cells across the model domain. Note that for both meteorological episodes, the increased urban land cover led to higher average (~ 0.3 and

Table 4

The average, standard deviation, and maximum hourly O₃ concentrations over non-water grid cells for the six MM5/CMAQ simulations

Simulation number	Average (standard deviation) (ppb)	Maximum (ppb)
1	45.62 (19.87)	141.8
2	46.02 (20.13)	143.4
3	44.55 (21.31)	137.1
4	41.55 (21.42)	146.9
5	41.84 (21.45)	150.2
6	40.33 (22.81)	155.2

0.4 ppb) and maximum (~1.6 and 3.3 ppb) O₃ concentrations compared to the respective base simulations. On the other hand, the cumulative effect of increased urban land cover, increased anthropogenic emissions that likely increased the titration of O₃ by NO_x, and decreased isoprene emissions led to lower average (~1 and 1.2 ppb) O₃ concentrations, but larger spatial and temporal variability as evidenced by the higher standard deviations. These findings illustrate the complex and often counteracting effects of substantial increases in urban cover across the domain on surface O₃ concentrations. On one hand, higher temperatures lead to increased radical production and photochemistry; however, higher PBL heights lead to increased pollutant dilution. Furthermore, we hypothesize that increased anthropogenic NO_x and decreased biogenic VOC emissions associated with increased urbanization have the potential to increase the spatial extent of VOC-limited conditions typically associated with core urban areas. In such areas, NO_x emissions contribute to decreased O₃ concentrations while they can lead to increased O₃ formation in downwind areas (e.g. Sillman, 1999). While no in-depth analysis has been performed to confirm this hypothesis, it is consistent with the spatial pattern of O₃ increases and decreases (see Fig. 5).

For the 1993 episode (simulation 1), 67.4% of the non-water grid cells had episode maximum 8 h O₃ concentrations exceeding 84 ppb. This increased to 71.0% and 78.0%, respectively, as the effects of urbanization alone (simulation 2) and the combined effects of urbanization and emissions changes (simulation 3) were considered. The 2056 episode, which had higher peak concentrations and included the effects of a different GCM scenario, experienced smaller incremental changes resulting from land use

change and combined land use/emissions changes. Simulations 4–6 (base, increased urbanization, and combined land use/emissions, respectively) resulted in 75.5%, 74.9%, and 77.1% of the grid cells having episode maximum 8 h O₃ concentrations exceeding 84 ppb.

Figs. 5a and b display maps of the episode-average O₃ concentrations for the 1993 (simulation 1) and 2056 (simulation 4) episodes; Figs. 5c and d display the changes in episode-average O₃ concentrations as a result of increased urban land cover for the two episodes (differences between simulations 2 and 1, and simulations 5 and 4); and Figs. 5e and f display the changes in episode-average O₃ concentrations as a result of both urban land cover change and anthropogenic emissions (differences between simulations 3 and 1, and simulations 6 and 4). For the 1993 base episode (simulation 1, Fig. 5a), the highest concentrations downwind of the NYC region occurred over Connecticut and Rhode Island, while large concentrations also occurred in the southwestern part of the model domain. The average concentrations across the domain during the 2056 episode (simulation 4, Fig. 5b) were lower, with peaks occurring over Long Island Sound, Delaware Bay/southern New Jersey, and Chesapeake Bay. The lowest O₃ concentrations occurred over the core urban area. In addition to the different spatial patterns in surface O₃ between the 1993 and 2056 base episodes, the domain-wide average O₃ over land was higher during the 1993 episode (60.7 ppb vs. 56.6 ppb).

Evident from Figs. 5c and d (effects of increased urban land cover alone) are increases in average O₃ concentrations across much of the NYC region, by 1–5 ppb. The changes in average O₃ were very small elsewhere, although there were a few areas outside of the core urban area where average O₃ decreased by ~1–3 ppb in the 2056 episode (simulation 5, Fig. 5d). The combined effects of increased urbanization and emissions changes are displayed in Figs. 5e and f, in which 1–7 ppb increases in O₃ are predicted over much of the non-water grid cells, while O₃ in the core NYC area and along the shore of Long Island Sound decreased by 3–5 ppb, likely a result of increased NO_x titration. Slight decreases are also visible in the Philadelphia region for this scenario, pointing to the existence of non-local impacts of land-use and emission changes made in the greater NYC area on this area of high existing emission density but without local changes in either land-use or emissions in our simulations. Over

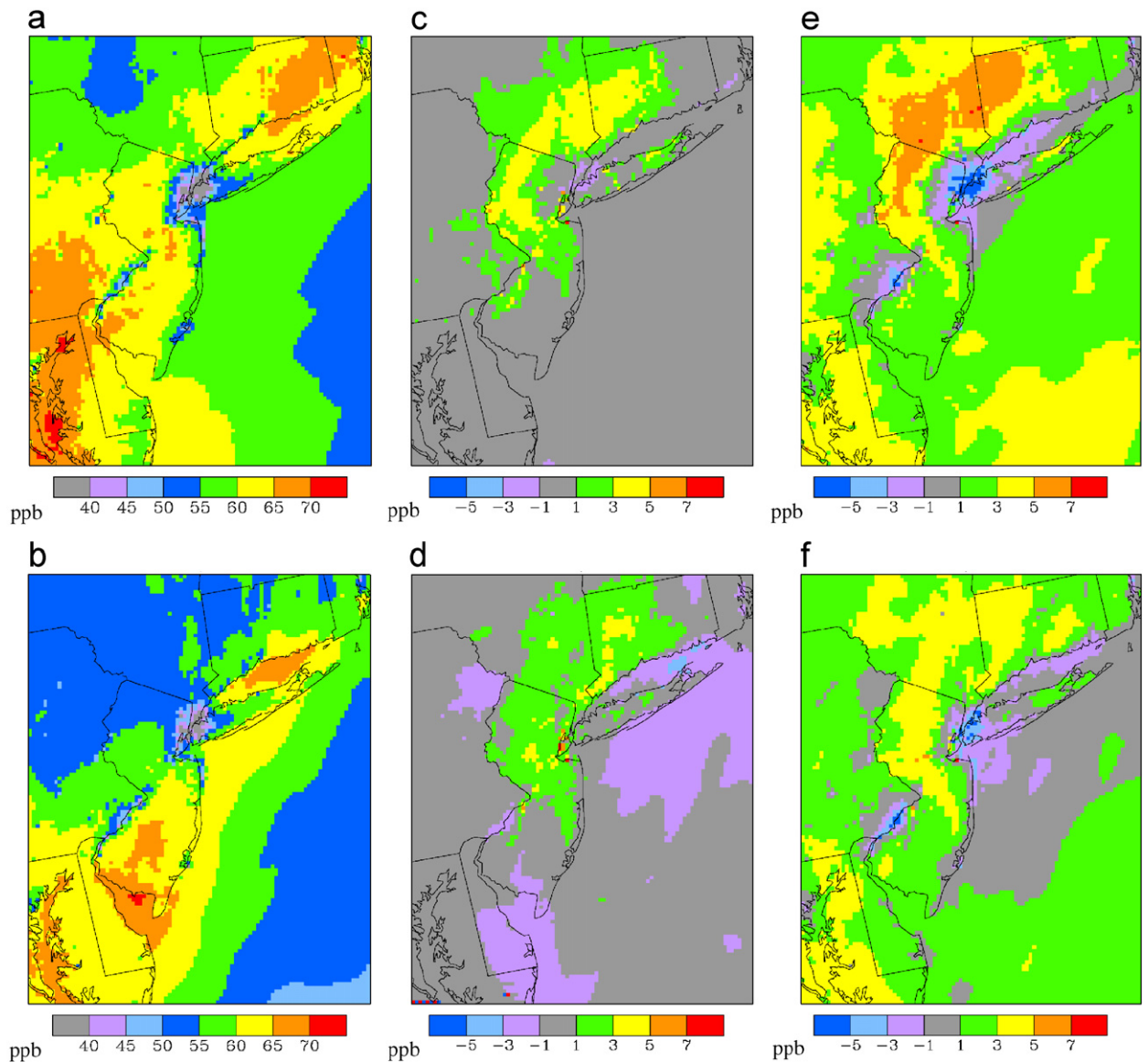


Fig. 5. Average surface O_3 concentrations for the; (a) base 1993 episode (simulation 1); and (b) base 2056 episode (simulation 4). Differences between the future model simulations and the respective base simulations, defined as “future-base”, (c) 1993 episode with 2050 A2 land use and 1990s emissions (simulation 2); (d) 2056 episode with 2050 A2 land use and 1990s emissions (simulation 5); (e) 1993 episode with 2050 A2 land use and 2050 A2 emissions (simulation 3); and (f) 2056 episode with 2050 A2 land use and 2050 A2 emissions (simulation 6).

northern New Jersey, southeastern New York, and western Connecticut, the increases in average surface O_3 were larger for the 1993 episode, as a result of increased urban land cover alone or increased urban land and anthropogenic emissions.

Fig. 6 displays the same information as in Fig. 5, except for episode-maximum 8 h O_3 for the two episodes. The effects are much more pronounced than with episode-average O_3 . For the 1993 episode

increased urbanization consistent with the A2 scenario led to 2–10 ppb increases in episode-maximum O_3 , corresponding to the areas outside of the core urban center. By comparison, increased urbanization alone led to large (> 14 ppb) increases in episode-maximum O_3 over Connecticut during the 2056 episode. Increases in surface O_3 of this magnitude would make compliance with air quality standards substantially more difficult. The com-

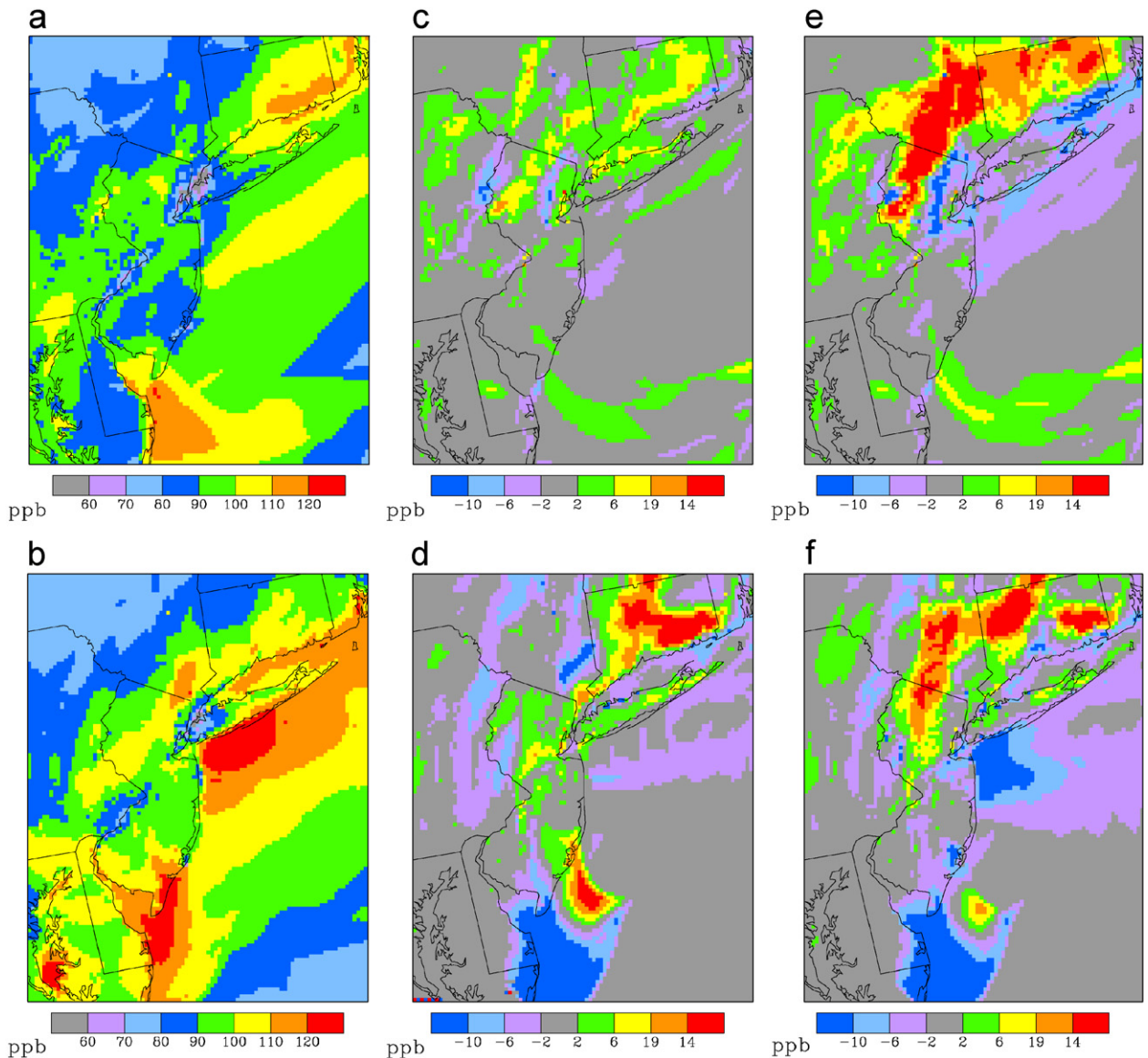


Fig. 6. Same as Fig. 6, except for episode maximum 8 h O₃ concentrations.

bin effects of urbanization and emissions changes led to even larger O₃ increases over the northern part of the domain, for both episodes. The changes in maximum O₃ over the core urban area were very small.

4. Discussion and summary

To our knowledge, this is the first time a successful attempt has been made to link and apply existing modeling systems to simulate the sensitivity of both meteorology and air quality to dynamic drivers across several scales likely to change in the

coming decades, such as global and regional climate, regional and local emissions, and local land-use. As such, this study lays the groundwork for future applications which might begin to “fill in” some of the missing pieces such as urbanization over larger areas or incorporating a direct feedback from meteorology on emissions. Furthermore, utilizing the system described here for sensitivity simulations even for relatively small areas may be of interest to planning organizations that focus on the state, county, or municipal level.

In this study we estimated the effects of future rates of urbanization and emissions in the NYC

metropolitan region on surface meteorology and O₃ concentrations. To this end, projections of future land use change and corresponding emissions changes assuming current technology and emission controls were integrated into the MM5/CMAQ modeling system and simulations were performed for two 18 day episodes at a horizontal resolution of 4 km. Results of our analysis suggest that extensive urbanization in the NYC area that is consistent with the narrative of the SRES A2 scenario has the potential to increase near-surface temperatures by more than 0.6 °C and PBL heights by more than 150 m, as well as decrease water vapor mixing ratio by more than 0.6 g kg⁻¹, during the afternoon hours in the NYC metropolitan area. The areal extent of all of these changes generally coincides with the area of increased urbanization. The results for surface temperature were similar to an earlier modeling study of extensive land cover change in this region (Civerolo et al., 2000). While substantial, these episode-average changes are still likely to be much smaller than might be expected from synoptic and seasonal variability, since meteorology can vary greatly from day to day and season to season.

In contrast to temperature, PBL heights, and water vapor, the impacts of these land use changes on ozone concentrations are more complex. Simulation results indicate that future changes in urbanization may lead to increases in episode-average O₃ levels by about 1–5 ppb, and episode-maximum 8 h O₃ levels by more than 6 ppb across parts of the NYC metropolitan area where urban growth is projected. However, spatial patterns of ozone changes are heterogeneous and also indicate the presence of areas with decreasing ozone concentrations. For example, episode-maximum 8 h O₃ levels decreased by 2 ppb or more in small areas outside the core urban center. When anthropogenic emissions were increased and biogenic emissions decreased to be consistent with the increased urbanization, the O₃ levels increased in outer counties of the metropolitan area but decreased in others (including coastal Connecticut and the Long Island Sound area, as well as over the Atlantic Ocean), likely at least in part due to the effects of increased titration. In the core urban center, increased urbanization alone had little effect on average or maximum O₃ concentrations, since the largest urban growth occurred in the outer counties. On the other hand, when emissions changes were included, the O₃ concentrations decreased in the core urban center as a result of titration processes.

Note that we did not examine near-surface winds in much detail, even though transport is clearly an important factor affecting O₃ levels. New York City is a large, heterogeneous urban area in a coastal region; wind patterns are highly complex as regional pollutant and precursor transport, sea breezes, and a substantial “heat island” play key roles. Increased urbanization did lead to an increased sea breeze in the vicinity of Long Island and coastal Connecticut (where O₃ generally decreased), and increasing convergence over southeastern New York and inland Connecticut (where O₃ generally increased). Future work should involve a more detailed examination of winds in this region.

Among the limitations of this study are the constraint of the simulated urbanization to the greater NYC area while leaving land use unchanged outside this area, and the simulation of only two relatively short time periods. Because the 2056 episode is not necessarily representative of the 1993 episode projected into the future it is not possible to directly include the effects of climate change in this study. However, despite these constraints the results presented here and in earlier studies (Solecki and Oliveri 2004; Hogrefe et al., 2004b; Kinney et al., 2006; Knowlton et al., 2004; Lynn et al., 2004) do illustrate the benefits of utilizing coupled modeling systems to quantitatively assess the potential air quality impacts of changes in climate, emissions and land use and their complex interaction. Using the framework described here, future studies could assess the impact of increased urbanization on climate and air quality over larger geographical areas and longer time periods.

Acknowledgments

This work was supported in part by the United States Environmental Protection Agency’s Science To Achieve Results (STAR) program under Grant R-82873301. The views expressed here do not necessarily reflect those of the supporting or participating agencies, and no official endorsement should be inferred.

References

- Aw, J., Kleeman, M.J., 2003. Evaluating the first-order effect of inter-annual temperature variability on urban air pollution. *Journal of Geophysical Research* 108, 4365.
- Bell, M., Ellis, H., 2003. Comparison of the 1 and 8 h national ambient air quality standards for ozone using models-3.

- Journal of the Air and Waste Management Association 53, 1531–1540.
- Bell, M., Ellis, H., 2004. Sensitivity analysis of tropospheric ozone to modified biogenic emissions for the mid-Atlantic region. *Atmospheric Environment* 38, 1879–1889.
- Binkowski, F.S., Roselle, S.J., 2003. Models-3 community multiscale air quality (CMAQ) model aerosol component—1, model description. *Journal of Geophysical Research* 108, 4183.
- Byun, D.W., Schere, K.L., 2006. Review of the governing equations, computational algorithms, and other components of the models—3/community multiscale air quality (CMAQ) modeling system. *Applied Mechanics Review* 59, 51–77.
- Carolina Environmental Programs, 2003. Sparse Matrix Operator Kernal Emissions (SMOKE) Modeling system. University of North Carolina, Chapel Hill, NC.
- Chen, F., Dudhia, J., 2001a. Coupling an advanced land-surface/hydrology model with the Penn State/NCAR MM5 modeling system: Part I—model implementation and sensitivity. *Monthly Weather Review* 129, 569–585.
- Chen, F., Dudhia, J., 2001b. Coupling an advanced land-surface/hydrology model with the Penn State/NCAR MM5 modeling system: Part II—preliminary model validation. *Monthly Weather Review* 129, 587–604.
- Civerolo, K.L., Sistla, G., Rao, S.T., Nowak, D.J., 2000. The effects of land use in meteorological modeling: implications for assessment of future air quality scenarios. *Atmospheric Environment* 34, 1615–1621.
- Claggett, P.R., Jantz, C.A., Goetz, S.J., Bisland, C., 2004. Assessing development pressure in the Chesapeake Bay Watershed: an evaluation of two land-use change models. *Environmental Monitoring and Assessment* 94, 129–146.
- Clarke, K.C., Hoppen, S., Gaydos, L., 1997. A self-modifying cellular automaton model of historical urbanization in the San Francisco Bay Area. *Environment and Planning B* 24, 247–261.
- Davies, H.C., Turner, R.E., 1977. Updating prediction models by dynamical relaxation: an examination of the technique. *Quarterly Journal of the Royal Meteorological Society* 103, 225–245.
- Dirmeyer, P.A., 2003. The role of the land surface background state in climate predictability. *Journal of Hydrometeorology* 4, 599–610.
- Dudhia, J., 1993. A nonhydrostatic version of the Penn State-NCAR Mesoscale model: validation tests and simulation of an Atlantic cyclone and cold front. *Monthly Weather Review* 121, 1493–1513.
- Gaza, R.S., 1998. Mesoscale meteorology and high ozone in the northeast United States. *Journal of Applied Meteorology* 37, 961–977.
- Geron, C.D., Guenther, A.B., Pierce, T.E., 1994. An improved model for estimating emissions of volatile organic compounds from forests in the eastern United States. *Journal of Geophysical Research* 99, 12773–12791.
- Gery, M.W., Whitten, G.Z., Killus, J.P., Dodge, M.C., 1989. A photochemical kinetics mechanism for urban and regional scale computer modeling. *Journal of Geophysical Research* 94, 12925–12956.
- Grell, G.A., Dudhia, J., Stauffer, D.R., 1994. A description of the fifth-generation Penn State/NCAR mesoscale model (MM5). Technical Note NCAR/TN-398+STR, National Center for Atmospheric Research, Boulder, CO, USA.
- Hogrefe, C., Lynn, B., Civerolo, K., Ku, J.-Y., Rosenthal, J., Rosenzweig, C., Goldberg, R., Gaffin, S., Knowlton, K., Kinney, P.L., 2004a. Simulating changes in regional air pollution over the eastern United States due to changes in global and regional climate and emissions. *Journal of Geophysical Research* 109, D22301.
- Hogrefe, C., Biswas, J., Lynn, B., Civerolo, K., Ku, J.-Y., Rosenthal, J., Rosenzweig, C., Goldberg, R., Kinney, P.L., 2004b. Simulating regional-scale ozone climatology over the eastern United States: model evaluation results. *Atmospheric Environment* 38, 2627–2638.
- Houyoux, M.R., Vukovich, J.M., Coats Jr., C.J., Wheeler, N.J.M., Kasibhatla, P., 2000. Emission inventory development and processing for the seasonal model for regional air quality (SMRAQ) project. *Journal of Geophysical Research* 105, 9079–9090.
- Kinney, P., Rosenthal, J., Rosenzweig, C., Hogrefe, C., Solecki, W., Knowlton, K., Small, C., Lynn, B., Civerolo, K., Ku, J., Goldberg, R., Oliveri, C., 2006. Chapter 6, assessing potential public health impacts of changing climate and land uses: the New York Climate & Health Project. In: Ruth, M., Donaghy, K., Kirshen, P. (Eds.), *Regional Climate Change and Variability: Impacts and Responses*. Edward Elgar, Cheltenham, UK, pp. 161–189.
- Knowlton, K., Rosenthal, J.E., Hogrefe, C., Lynn, B., Gaffin, S., Goldberg, R., Rosenzweig, C., Civerolo, K., Ku, J.-Y., Kinney, P.L., 2004. Assessing ozone-related health impacts under a changing climate. *Environmental Health Perspectives* 112, 1557–1563.
- Ku, J.-Y., Mao, H., Zhang, K., Civerolo, K., Rao, S.T., Philbrick, C.R., Doddridge, B., Clark, R., 2001. Numerical investigation of the effects of boundary-layer evolution on the prediction of ozone and the efficacy of emission control options in the northeastern United States. *Environmental Fluid Mechanics* 1, 209–233.
- Luley, C.J., Bond, J., 2002. A plan to integrate management of urban trees into air quality planning. Report to the North East State Foresters Association (available at http://www.treescleanair.org/policymakers/studies/IntegrateTrees_LuleyBond.pdf).
- Lynn, B.H., Druyan, L., Hogrefe, C., Dudhia, J., Rosenzweig, C., Goldberg, R., Rind, D., Healy, R., Rosenthal, J., Kinney, P., 2004. Sensitivity of present and future surface temperatures to precipitation characteristics. *Climate Research* 28, 53–65.
- Lynn, B.H., Rosenzweig, C., Goldberg, R., Hogrefe, C., Rind, D., Healy, R., Dudhia, J., Biswas, J., Druyan, L., Kinney, P., Rosenthal, J., 2006. The GISS-MM5 regional climate modeling system: part 1—sensitivity of simulated current and future climate to model configuration. *Journal of Applied Meteorology*, Submitted for publication.
- Mebust, M.R., Eder, B.K., Binkowski, F.S., Roselle, S.J., 2003. Models-3 community multiscale air quality (CMAQ) model aerosol component, 2, model evaluation. *Journal of Geophysical Research* 108, 4184.
- National Research Council, 1991. *Rethinking the Ozone Problem in Urban and Regional Air Pollution*. National Academy Press, 500pp.
- Pozzi, F., Small, C., 2005. Analysis of urban land cover and population density in the United States. *Photogrammetric Engineering and Remote Sensing* 71, 719–726.
- Rao, S.T., Ku, J.-Y., Berman, S., Zhang, K., Mao, H., 2003. Summertime characteristics of the atmospheric boundary

- layer and relationships to ozone levels over the eastern United States. *Pure and Applied Geophysics* 160, 21–55.
- Russell, G.L., Miller, J.R., Rind, D., 1995. A coupled atmosphere-ocean model for transient climate change studies. *Atmosphere–Ocean* 33, 683–730.
- Sillman, S., 1999. The relation between ozone, NO_x , and hydrocarbons in urban and polluted rural environments. *Atmospheric Environment* 33, 1821–1845.
- Solecki, W.D., Oliveri, C., 2004. Downscaling climate change scenarios in an urban land use change model. *Journal of Environmental Management* 72, 105–115.
- Tong, D.Q., Mauzerall, D.L., 2006. Spatial variability of summertime tropospheric ozone over the continental United States. *Atmospheric Environment* 40, 3041–3056.
- United States Environmental Protection Agency (US EPA), 1994. User's guide to mobile5 (mobile source emission factor model). Report EPA/AA/TEB/94/01, Ann Arbor, MI.
- Williams, E.J., Guenther, A., Fehsenfeld, F.C., 1992. An inventory of nitric oxide emissions from soils in the United States. *Journal of Geophysical Research* 97, 7511–7519.